

Formation and Thermal Stability of Nickel Germanide on Germanium Substrate

Qingchun ZHANG, Nan WU, Thomas OSIPOWICZ², Lakshmi Kanta BERA¹ and Chunxiang ZHU*

Silicon Nano Device Laboratory, Department of Electrical and Computer Engineering, National University of Singapore, 10 Kent Ridge Crescent, Singapore 119260

¹*Institute of Microelectronics, Singapore 117685*

²*Department of Physics, Faculty of Science, National University of Singapore, 10 Kent Ridge, Singapore 119260*

(Received August 16, 2005; accepted September 23, 2005; published October 28, 2005)

The formation and thermal stability of nickel germanide on germanium substrate were examined by both electrical and physical characterization methods. Low resistivity ($14\ \mu\Omega\ \text{cm}$) mono-nickel–germanide was formed at a low temperature of 400°C on Ge substrate. The sheet resistance of nickel germanide changed with the germanide formation temperatures and had a similar characteristic as nickel silicide. However, the thermal stability study shows that NiGe formed on Ge substrate has a poorer thermal stability than NiSi on Si substrate, which is due to the lower activation energy of agglomeration in NiGe ($2.2 \pm 0.2\ \text{eV}$) compared to NiSi. [DOI: 10.1143/JJAP.44.L1389]

KEYWORDS: nickel germanide, thermal stability, activation energy

Germanium is always an interesting material for metal oxide semiconductor field effect transistor (MOSFET) applications because of its high intrinsic mobility (two times higher for electrons and four times higher for holes as compared to those in Si). However, the inferior thermal stability and water solubility of germanium oxide hinder the real application of Ge MOSFET. Owing to recent developments of replacing high dielectric constant (high- k) material over thermally grown SiO_2 as a new gate dielectric in Si complementary metal oxide semiconductor (CMOS) devices, Ge as a channel material has attracted a great interest for high-performance logic circuit application. Ge MOSFETs with germanium oxynitride, ZrO_2 and HfO_2 dielectrics have been successfully demonstrated.^{1–3)} However, very high series resistance was observed in these Ge MOSFETs, which severely degraded the device performance. Self-aligned silicide is essential in current deep-sub micron very-large-scale-integration (VLSI) circuit fabrication to reduce the parasitic resistance. Titanium silicide (TiSi_2), cobalt silicide (CoSi_2) and nickel silicide (NiSi) have been extensively studied. Titanium silicide was widely used in sub-micron CMOS technologies, however, it has been replaced by cobalt silicide for the sub $0.25\ \mu\text{m}$ nodes. Ni silicide, considered as the material choice for the future nodes, has several advantages over Ti silicide and Co silicide which include: low temperature silicidation, no bridging failure property, small mechanical stress, low silicon consumption, and one step silicidation process.⁴⁾ Similarly, Ni shows advantages to form germanide for Ge MOSFET application over other materials. It has been reported that high processing temperatures are required to form low-resistivity titanium germanide ($>800^\circ\text{C}$) and cobalt germanide ($>500^\circ\text{C}$), while nickel germanide can be formed at a low temperature of 270°C .⁵⁾ Such a low processing temperature is effective to prevent the degradation of high- k gate stack on germanium substrate and makes nickel germanide more suitable for Ge device fabrication.

In this work, the formation of nickel germanide on single crystal germanium substrate by rapid thermal processing (RTP) is investigated over a wide range of temperatures (250 – 700°C). Thermal stability is studied using electrical

(sheet resistance measurement) and physical (scanning electron microscopy, SEM) characterization methods. Activation energy of morphological degradation due to agglomeration is determined for NiGe on single crystalline germanium substrate.

NiGe formation was carried out on n-type (0.45 – $0.51\ \Omega\ \text{cm}$) (100) germanium substrates. First, the substrates were dipped in diluted HF solution (1 : 20) to remove the native oxide and passivate the surface with hydrogen. After that, the substrates were transferred into an E-beam evaporator with a base pressure of 5×10^{-7} mbar. Ni films with different thicknesses were deposited at room temperature. Following that, nickel germanide was formed by RTP at temperatures ranging from 250 to 700°C under N_2 at atmosphere. After annealing, the unreacted Ni was removed by diluted HNO_3 (1 : 20). To study the thermal degradation behavior, several NiGe samples, formed at the same condition (400°C , 30 s), were subsequently annealed at different temperatures from 450 to 650°C . A four-point probe was used to measure the sheet resistance of the nickel germanide films. Rutherford backscattering spectroscopy (RBS), with a 2 MeV He^+ ion beam of approximate $5\ \text{m}^2$ raster-scanned over a square pad of $50 \times 50\ \mu\text{m}^2$, was used to measure the thicknesses of as-deposited Ni and Ni germanide films as well as the film composition. SEM was employed to examine the morphology of the films.

Nickel germanide formation was first studied over a wide range of temperatures. Figure 1 shows the sheet resistance (R_{sh}) of nickel germanide as a function of annealing temperature with Ni film thickness (nominal) of 10 and 20 nm. For comparison, the sheet resistance of the silicide formed by reaction of nominal 20 nm Ni on single crystal silicon is also characterized and shown in Fig. 1. The curves of the germanide sheet resistance on Ge substrate seem similar to that of silicide on Si substrates. All the films exhibit high sheet resistances at low temperatures due to the formation of Ni-rich phases (predominantly Ni_2Si or Ni_2Ge).^{4,6)} At elevated temperatures, the sheet resistance maintains at a minimum value over a range of temperatures (400 – 550°C for germanide, 400 – 700°C for silicide with 20 nm Ni). The resistivity of NiGe is extracted to be $14\ \mu\Omega\ \text{cm}$, which is comparable with the resistivity of NiSi ($14\ \mu\Omega\ \text{cm}$) but is lower than the resistivity of NiSiGe

*E-mail address: elezhucx@nus.edu.sg

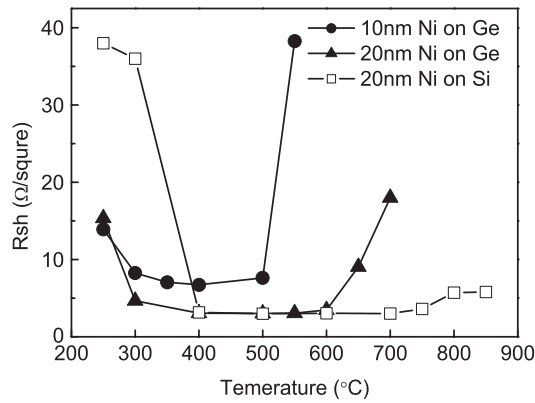


Fig. 1. The sheet resistance of NiGe formed at temperatures ranging from 250 to 700°C for 30 s. The sheet resistance was measured after removing the unreacted Ni by wet etching after reaction. The nominal 10 and 20 nm Ni films were deposited on (100) single crystalline Ge and Si substrates.

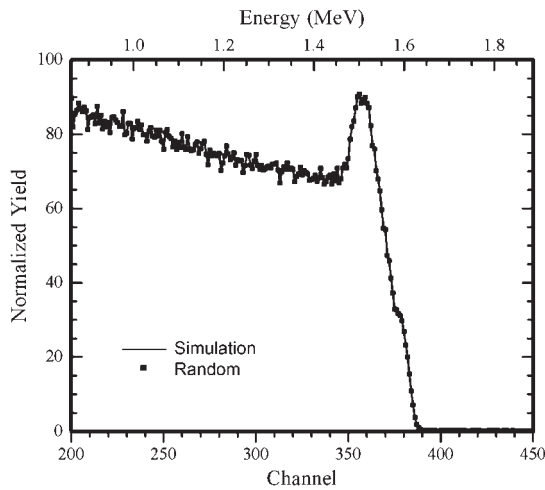


Fig. 2. RBS spectrum of NiGe formed at 500°C with nominal 20 nm initial Ni. From the simulation curves of RBS data, the sample composition maintains a constant as Ni : Ge = 1 : 1.

($18 \mu\Omega \text{ cm}$).^{7,8)} The low sheet resistance within this temperature range indicates that mono-germanide and mono-silicide were formed. The RBS analysis confirms that the atomic ratio of Ge to Ni is 1 : 1 corresponding to mononickel-germanide (Fig. 2). RBS was also employed to measure the thickness of formed germanide film. The thickness ratio of the NiGe films to the as-deposited Ni films is 2.55, from a series of NiGe samples with different as-deposited Ni thickness. When the annealing temperature increases further, a sharp and slight increase in the sheet resistance (R_{sh}) of NiGe and NiSi were observed due to the thermal degradation of germanide and silicide, respectively. It is noticed that the thermal degradation of germanide films occur at lower temperatures than that of NiSi films (Fig. 1). Hsu *et al.* reported similar results on NiGe on single- and poly crystalline Ge substrates.⁹⁾

It is well known that the thermal degradation of NiSi at high temperature includes two mechanisms: agglomeration and phase transformation.⁷⁾ The desired low-resistivity phase NiSi tends to transform to high-resistivity NiSi₂ above 700°C which accounts for the high sheet resistance plateau around 800°C. Further increasing annealing temperature will

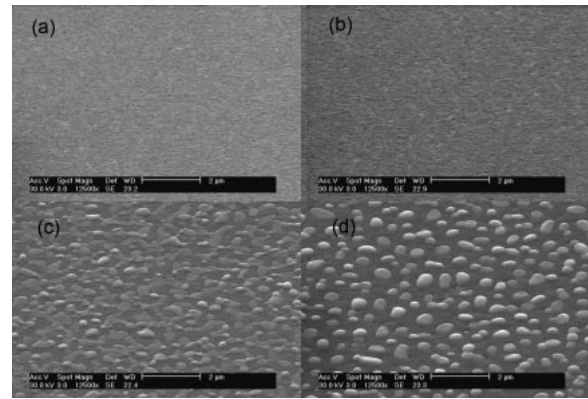


Fig. 3. SEM pictures of nickel germanide formed at annealing temperature of (a) 400, (b) 500, (c) 600, and (d) 700°C. The initial Ni thickness is 15 nm.

cause the initial continuous silicide film to break up into discrete silicide islands. In contrary, the NiGe shows a different degradation characteristic with NiSi. The nickel germanide does not transform to Ge-rich phase after annealing since no Ge-rich phase (>50 at. % Ge) exists in the equilibrium phase diagram.¹⁰⁾ Morphological degradation due to the agglomeration is the only mechanism of thermal degradation in NiGe. The agglomeration in NiGe starts with grain boundary grooving and results in islands formation, as the same as silicide agglomeration.¹¹⁾ The agglomeration is driven by the minimization of the total surface/interface energy of the germanide and germanium substrate.¹²⁾ Figure 3 shows the SEM pictures of NiGe films formed with different annealing temperatures. Combining the sheet resistance curves shown in Fig. 1, the keeping increasing sheet resistance with the annealing temperature is due to the severe agglomeration until it thermally breaks into discrete islands. In addition, it is noted from Fig. 1 that the temperature at which agglomeration occurs decreases with reduced film thickness. This is also consistent with the grooving model of agglomeration.

The dependence of thermal stability of NiGe on both annealing temperature and time was studied by monitoring the sheet resistance variation. The germanide films were first formed by the same RTP condition (400°C, 30 s). Following that, the samples were subsequently annealed at different temperatures and durations. Figure 4 shows the sheet resistance ratio ($R_{\text{sh}}/R_{\text{sh0}}$) of NiGe, formed with 10 and 20 nm Ni on Ge substrates, as a function of annealing time at varying temperatures, where R_{sh0} is the initial sheet resistance value measured after NiGe formation annealing and R_{sh} is the sheet resistance measured after the second annealing. All the sheet resistance ratios increase with annealing time at different annealing temperatures. A higher annealing temperature leads to a faster increase in $R_{\text{sh}}/R_{\text{sh0}}$. These results are consistent with the morphological degradation due to agglomeration. To further characterize the thermal degradation of NiGe, the activation energy of agglomeration was estimated. Figure 5 shows the Arrhenius plots of $\ln \tau_0(T)$ as a function of $1/kT$ for NiGe formed with 10 and 20 nm Ni on germanium substrates, where $\tau_0(T)$ is degradation time defined as the time at a given temperature (T) corresponding to a 20% increase in sheet resistance (R_{sh})

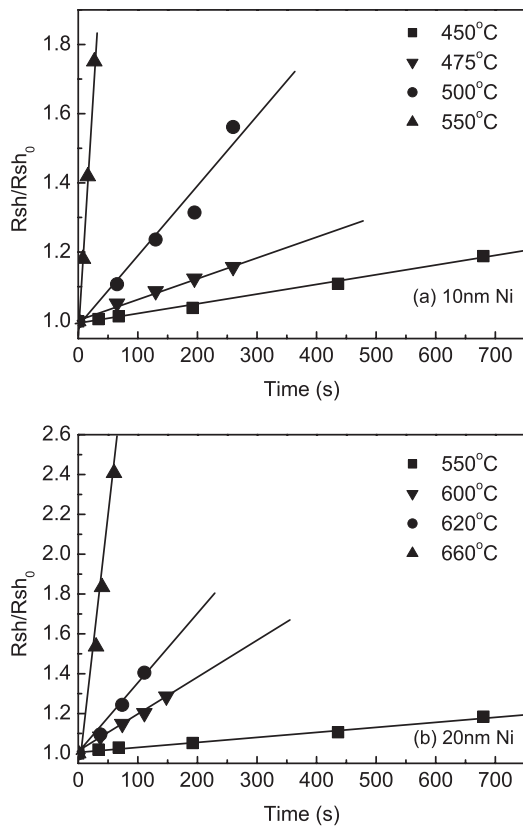


Fig. 4. Evolution of NiGe sheet resistance with annealing time for samples with (a) 10 and (b) 20 nm as-deposited Ni.

from its initial sheet resistance (R_{sh0}). From Fig. 5, the activation energy of NiGe agglomeration is estimated to be 2.2 ± 0.2 eV. The activation energy value of NiGe agglomeration is smaller than the reported values of NiSi. By measuring the degradation of sheet resistance of NiSi films, Chamirian *et al.* reported the activation energy values to be 2.5 ± 0.25 eV and 2.6 ± 0.3 eV for the n+ and p+ Si(100) substrates, respectively.¹³⁾ Colgan *et al.* also reported that the activation energy of the NiSi agglomeration was 2.9 ± 0.2 eV with the same method.¹⁴⁾ Okubo *et al.* reported activation energy at 2.8 ± 0.4 eV by calculating exposed-Si area.¹⁵⁾ They suggested that the activation energy of NiSi agglomeration corresponds to the energy needed for adding a Si atom to the epitaxial Si that grows between NiSi grains. The lower activation energy of the NiGe agglomeration could be attributed to the lower activation energy of Ge epitaxy than Si epitaxy.¹⁶⁾

In summary, the formation and thermal stability of NiGe were examined. Low resistivity ($14 \mu\Omega$ cm) NiGe was formed at a low temperature of 400°C . The NiGe shows a poorer thermal stability than NiSi. The agglomeration in NiGe accounts for the thermal degradation after high

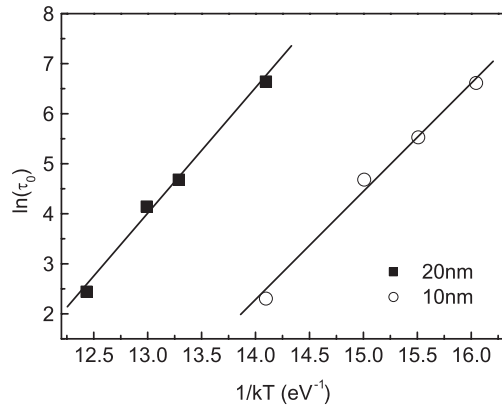


Fig. 5. Arrhenius plots of degradation time for NiGe films with 10 and 20 nm as-deposited Ni. The degradation time is defined as corresponding to a 20% increase in sheet resistance.

temperature annealing with the activation energy of 2.2 ± 0.2 eV.

Acknowledgment

The work was supported by Singapore ASTAR grant R-263-000-267-305.

- 1) H. Shang, K.-L. Lee, P. Kozlowski, C. D'Emic, I. Babich, E. Sikorshi, M. Jeong, H.-S. P. Wong, K. Guarini and W. Haensch: IEEE Electron Device Lett. **25** (2004) 135.
- 2) H. Shang, H. Okorn-Schmidt, K. K. Chan, M. Copel, J. A. Ott, P. M. Kozlowski, S. E. Steen, S. A. Cordes, H.-S. P. Wong, E. C. Jones and W. E. Haensch: IEDM Tech. Dig., 2002, p. 441.
- 3) C. O. Chui, H. Kim, P. C. McIntyre, K. C. Saraswat: IEDM Tech. Dig., 2003, p. 18.3.1.
- 4) T. Morimoto, T. Ohguro, H. S. Momose, T. Inuma, I. Kunishima, K. Suguro, I. Katakabe, H. Nakajima, M. Tsuchiaki, M. Ono, Y. Katsumata and H. Iwai: IEEE Trans. Electron Devices **42** (1995) 915.
- 5) S. P. Ashburn, M. C. Ozturk, J. J. Wortman, G. Harris, J. Honeycutt and D. M. Maher: J. Electron. Mater. **21** (1992) 81.
- 6) M. Wittmer, M.-A. Nicolet and J. W. Mayer: Thin Solid Films **42** (1997) 51.
- 7) E. G. Colgan, M. Maenpaa, M. Finetti and M.-A. Nicolet: J. Electron. Mater. **12** (1983) 413.
- 8) C. Isheden, J. Seger, H. H. Radamson, S.-L. Zhang and M. Östling: Mater. Res. Soc. Symp. Proc. **745** (2003) N4.9.1.
- 9) S.-L. Hsu, C.-H. Chien, M.-J. Yang, R.-H. Huang, C.-C. Leu and S.-W. Shen: Appl. Phys. Lett. **86** (2005) 251906.
- 10) A. Nash and P. Nash: Bull. Alloy Phase Diagrams **8** (1987) 255.
- 11) K. Y. Lee, S. L. Liew, S. J. Chua, D. Z. Chi, H. P. Sun and X. Q. Pan: Mater. Res. Soc. Symp. Proc. **810** (2004) 55.
- 12) J. P. Gambino and E. G. Colgan: Mater. Chem. Phys. **52** (1998) 99.
- 13) O. Chamirian, J. A. Kittl, A. Lauwers, O. Richard, M. van Dal and K. Maex: Microelectron. Eng. **70** (2003) 201.
- 14) E. G. Colgan, J. P. Gambino and B. Cunningham: Mater. Chem. Phys. **B 46** (1996) 209.
- 15) K. Okubo, Y. Tsuchiya, O. Nakatsuka, A. Sakai, S. Zaima and Y. Yasuda: Jpn. J. Appl. Phys. **43** (2004) 1896.
- 16) O. Hellman: Mater. Sci. Eng. R **16** (1996) 1.